*Progress In Electromagnetics Research C, Vol. 132, 145–157, 2023*

# Concentric Circular Antenna Array Synthesis Using Advanced Marine Predator Algorithm

**Eunice O. Owoola[1], Kewen Xia[1, *], Victor O. Adewuyi[2], and Paul S. Kanda[1]**

**Abstract**—In antenna design, the low side lobe level (SLL) of the antenna radiation pattern plays a crucial role in communication systems as it reduces signal interference along the entire side lobes of the radiation pattern. This paper presents an effective technique to minimize the SLL and thus improve the radiation pattern of the concentric circular antenna array (CCAA) using an advanced marine predator algorithm (AMPA). The AMPA is inspired by the predator-prey relationship in aquatic ecosystems, and it incorporates an improved adaptive velocity update strategy and a chaotic sequence parameter. In this work, the AMPA is applied to synthesize two examples of CCAA (4,6,8-CCAA elements and 8,10,12-CCAA elements) under two different instances (without and with a centre element). The simulation results achieved a significant improvement in SLL minimization as compared to the uniform array, standard marine predator algorithm (MPA), and some other nature-inspired metaheuristic algorithms.

## 1. INTRODUCTION

Designing antennas with relatively high directional properties is important in addressing the requirement of antennas used for long-distance communication. In addition, to effectively achieve improved directional properties such as high gains and enlarged electrical size, radiating elements are assembled in an electrical and geometrical configuration such that their field patterns in the desired direction are constructive and destructive in the other directions [1, 2]. Some of the benefits of this configuration include lower side lobe level (SLL) with a very high directive pattern. Another benefit is the efficient control over the direction of steer of the array radiation pattern towards the best signal path, and this is accomplished by varying the number of elements, excitation coefficients, inter-element spacing, relative phases, and overall array geometrical arrangement (linear, rectangular, circular, elliptical ones, etc.)

Linear arrays, which are popular for their simplicity of design and high directivity of the main lobe in a specific direction [2], have the drawback of inefficient radiation across 360-degree azimuthal directions. In circular arrays, the absence of edge elements allows for the electronic rotation of the array without deforming the radiation pattern, and its main lobe can be channeled and focused in any direction throughout the entire space by rotating 360 degrees [3]. The concentric circular rings of different radii, known as concentric circular antenna array (CCAA), find extensive applications in modern communications systems because of their strength compared to the linear and rectangular array. Some notable merits of the CCAA include 360-degree-azimuth scanning, coverage of invariant angle, ease of pattern synthesis, effective spectrum utilization, low mutual coupling sensitivity, etc.

The optimal design of the antenna array, which usually involves minimizing the SLL, is vital in reducing unwanted radiation beams from the electromagnetic transmission [4]. A low SLL and a narrow first null beamwidth (FNBW) are some of the main parameters of interest when antenna arrays are designed. Generally, many synthesis techniques focus on suppressing unwanted signals by

*Received 16 February 2023, Accepted 10 April 2023, Scheduled 24 April 2023*
* Corresponding author: Kewen Xia (kwxia@hebut.edu.cn).
[1] School of Electronics and Information Engineering, Hebei University of Technology, Tianjin 300401, China. [2] School of Electronics and Information Engineering, Changchun University of Science and Technology, Changchun 130022, China.

minimizing the SLL [5–8]. The application of evolutionary optimization algorithms in solving complex engineering problems, especially in array synthesis, is widely explored in the literature. These include genetic algorithm (GA), simulated annealing (SA), gravitational search algorithm (GSA), particle swarm optimization (PSO), etc. To optimize CCAAs, Mandal et al. developed a particle swarm optimization (PSO) with a constriction factor (PSOCFA) [9]. The backtracking search optimization method (BSA) was used by Guney et al. [10] to synthesize CCAAs with minimized SLLs at a constant beamwidth. Hybrid Antlion and Grasshopper Optimization Algorithms have been used by Amaireh et al. to lower the SLL of circular antenna arrays [3]. Circular and concentric circular antenna arrays are designed using cat swarm optimization (CSO) [11]. Hybrid adaptive differential evolution and particle swarm optimization (ADEPSO) was put out by Ram et al. to enhance the directivity of time-modulated CCAAs [12].

An opposition-based Bat method was suggested by Ram et al. to create the best CCAA with enhanced radiation properties [13]. CCAAs are designed using a nature-inspired optimization method known as the dragonfly algorithm (DA), which yields reduced side lobes [14]. A moth flame optimization (MFO) technique was suggested by Das et al. to enhance the CCAAs' radiation pattern [15]. The SLL of CCAA radiation patterns was decreased by using the Symbiotic Organisms Search (SOS) method [16], and also Bera et al. adopted a hybrid GSA and PSO for the same purpose [2]. A Cuckoo search-based hybrid technique was used by Sun et al. to synthesize the radiation beam patterns of CCAAs [17]. High-altitude platform CCAAs have been given a performance boost using comprehensive learning PSO [18]. To reduce the SLL of CCAAs considering mutual coupling, ant lion optimization (ALO) has been suggested [19]. For the optimization of phase-only reconfigurable CCAA, SOS is employed [20].

Recently, a new metaheuristic technique called advanced marine predator algorithm (AMPA), which is an improvement of the standard marine predator algorithm (MPA) has been proposed for several kinds of solving optimization problems [8]. The standard MPA, though efficient in solving some engineering problems [8, 21, 22], fails to generate a diversified initial population with good efficiency, escapes from the local optimum slowly, and explores a limited search space [23, 24]. The AMPA proposed by Owoola et al. [8] incorporates an improved velocity and position update into the MPA to improve its exploration ability and mitigate the MPA's stagnancy problem. The Chebyshev map is also included to help with the velocity and thus improve the algorithm's exploitation capacity. The AMPA has been used to synthesize the circular antenna array (CAA), and it outperforms some other metaheuristic algorithms in suppressing the CAA's SLL with an enhanced convergence rate [8]. However, it is yet to be applied to CCAA pattern synthesis.

In this paper, the AMPA is applied for the SLL minimization of CCAA for the first time. The goal of this work is to investigate and observe the efficacy of the AMPA technique, as well as to determine the excitations of the ring elements that satisfy the radiation pattern constraints. The AMPA's effectiveness and stability are tested on four different examples of CCAA, and the results obtained by AMPA are compared to those gotten by existing methods such as MPA, non-linear MPA, invasive weed optimization (IWO), moth flame optimization (MFO) algorithm, arithmetic optimization algorithm (AOA), and grey wolf optimization (GWO).

The arrangement of this paper is as follows. Section 2 describes the array factor formulation of the CCAA and also the objective function of the CCAA synthesis. In Section 3, a brief description of the AMPA is presented. The performance analysis of AMPA and the comparison with several existing optimization algorithms for the synthesis of CCAAs are provided in Section 4. Finally, Section 5 concludes the paper.

## 2. THE GEOMETRY AND PROBLEM FORMULATION

### 2.1. The CCAA Model

Figure 1 depicts the configuration of a concentric circular antenna array (CCAA), with $X$ concentric rings of antenna and radius $r_X$ having $N_X$ number of isotropic elements in ring $X$. The radiation pattern of the CCAA can be written in terms of the array factor:

$$F(\theta, \varphi) = I_C + \sum_{x=1}^{X} \sum_{i=1}^{N_x} I_{xi} \exp\left[jkr_x \sin\theta \cos(\varphi - \varphi_{xi}) + \alpha_{xi}\right]. \quad (1)$$

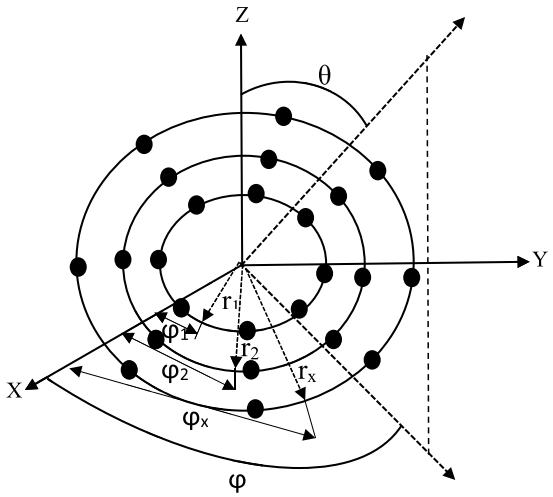


**Figure 1.** The CCAA structure.

$$\varphi_{xi} = \frac{2\pi i}{N_x}. \tag{2}$$

$$\alpha_{xi} = -kr\sin(\theta_0)\cos(\varphi_0 - \varphi_{xi}). \tag{3}$$

where $F$, $I_c$, $I_{xi}$, and $\alpha_m$ are the array factor, the excitation of the centre element, the excitation of the $i$th element in the $x$th ring, and the phase of the $i$th element in the $x$th ring. $\theta$ and $\varphi$ are the azimuth and elevation angles, respectively.

### 2.2. The Problem Formulation

The goal of this work is to suppress the CCAA's SLL by optimizing its excitation amplitude at specific inter-element spacing. Therefore, the cost function is written as [8]:

$$f = w \times \left(\max\left(F(\theta_{\text{PSL}}^{R_1})\right) + \max\left(F(\theta_{\text{PSL}}^{R_2})\right)\right) \tag{4}$$

where $w$ is the weight, and $\theta_{\text{PSL}}^{R_1}$ and $\theta_{\text{PSL}}^{R_2}$ are the peak SLL minimization angles. The equation minimizes the SLL of the CCAA's radiation pattern; thus, the optimization problem is expressed as:

$$\min \ f(I_1, I_2, I_3, ....., I_n). \tag{5}$$

$$s.t. \ \ \theta_{\text{PSL}}^{R} = \in \max\left([-\pi, \theta_{R1}] \cup [\theta_{R2}, \pi]\right). \tag{6}$$

$$0 \leq I_n < 1, \ \ n = 1, 2, 3, ....., N \tag{7}$$

where $[-\pi, \theta_{R1}]$ and $[\theta_{R2}, \pi]$ represent the sections of the SLL minimization.

## 3. THE METAHEURISTIC ALGORITHM EMPLOYED

### 3.1. The Marine Predators Algorithm (MPA)

The marine predator algorithm (MPA) is governed by different foraging strategies among aquatic predators and prey, as well as their optimal encounter rates procedure in biological interaction. The optimal foraging strategies used in this algorithm are based on the Lévy flight and Brownian motion. The standard MPA optimization stage is divided into three phases based on predator and prey movement strategies and velocity. The prey's update velocity in each phase is determined based on the following three conditions. The first instance is when the predator moves faster than the prey; the second case is when the prey moves faster than the predator; and the last condition is when the prey and predator move at almost the same pace. The full description of MPA is described in [21].

### 3.2. The Advanced Marine Predator Algorithm (AMPA)

In the initialization phase, a population of the random solution (Prey) is generated, and the best-obtained solution named 'top predator' is considered for the optimization phase. The top predator is used to construct a matrix called Elite as shown in Equation (8).

$$Elite = \begin{bmatrix} X_{1,1} & X_{1,2} & ..... & X_{1,d} \\ X_{2,1} & X_{2,2} & ..... & X_{2,d} \\ \vdots & \vdots & \vdots & \vdots \\ X_{n,1} & X_{n,2} & ..... & X_{n,d} \end{bmatrix}_{n\times d} \tag{8}$$

where $n$ and $d$ represent the search-number agent or population size and the dimension, respectively. $X$ is the top predator. The Elite is updated based on the optimal solution gotten during the optimization phase in each iteration. The initialization stages of the MPA and AMPA are similar. The major difference between the two algorithms lies in the optimization procedure.

#### *3.2.1. Optimization Stage*

The optimization process of AMPA explores the search area randomly on several areas and approaches to find a better solution based on the exploration and exploitation approach. This process has two phases which are decided by a "pass" value set within the algorithm. The pass value in this work is set to 0.6, and the algorithm executes the optimization process as stated in Equation (9).

$$\text{Optimization process} = \begin{cases} \textit{Phase 1} & \text{if rand} < \text{pass} \\ \textit{Phase 2} & \text{if rand} > \text{pass} \end{cases} \tag{9}$$

*Phase 1:* In the first phase, the formula for the prey's velocity update with respect to the predator is described in Equation (12). This equation takes the place of the first three phases of the standard MPA, and it proffers a better solution because it considers both the personal best solution of each prey and their global best solution. The global best solution is constructed into a matrix form called Elite. This enables the algorithm's exploration capacity to be expanded. The velocity update employed in this technic is expressed as:

$$\overrightarrow{V_{i,j}} = A \times \overrightarrow{V_{i,j}} + b_1 e^{-\beta r_p^2}(pbest_{i,j} - Prey_{i,j}) + b_2 e^{-\beta r_g^2}(gbest_{i,j} - Prey_{i,j}) \tag{10}$$

$$r_p = norm(pbest_{i,j} - Prey_{i,j}) \tag{11}$$

$$r_g = norm(EliteP - Prey_{i,j}) \tag{12}$$

where $V$, $\beta$, and $A$ represent the velocity, distance sight coefficient, and adaptive weight, respectively. $b_1$ and $b_2$ symbolize the learning coefficients. *gbest* and *pbest* are the global best position and personal best position, respectively. *EliteP* is the same as the global best position or Elite position.

The updated Prey is consequently stated as:

$$\overrightarrow{Prey_{i,j}} = \overrightarrow{Prey_{i,j}} + P \times C \times \overrightarrow{V}_{i,j} \tag{13}$$

where $P$ is a constant value that equals 0.4 in this work. The chaotic map adopted in this research is the Chebyshev map, and its coefficient is represented as $C$.

*The Chebyshev map:* This is a one-dimensional chaos map with a straightforward iterative equation. It has pseudo-random output sequences, a high stochastic property, and is parameter-sensitive and initial value sensitive [25]. It is expressed mathematically as [25]:

$$x_{s+1} = \cos(k \cos^{-1}(x_s)) \tag{14}$$

The Chebyshev map is used in this work to create chaotic orders that can enhance the velocity and thus the exploitation capability and convergence of the technique. For the Chebyshev map, the starting value is 0.7, and the number of iterations is 100.

*Phase 2:* This next phase of AMPA is similar to the final phase of the standard MPA. This scenario occurs when the predator moves faster than the prey with high exploitation capability. The equation

for the updated velocity and prey is given as:

$$\begin{aligned} \overrightarrow{V}_{i,j} &= \overrightarrow{r}_l \otimes \left( \overrightarrow{r}_l \otimes \overrightarrow{Elite}_{i,j} - \overrightarrow{Prey}_{i,j} \right) \\ \overrightarrow{Prey}_{i,j} &= \overrightarrow{Elite}_{i,j} + \left( P \times AP \otimes \overrightarrow{V}_{i,j} \right) \end{aligned} \tag{15}$$

The movement of the predator is Lévy, and it can be expressed mathematically as:

$$\overrightarrow{r}_l = 0.05 * \left( \frac{N_{randn} \times \delta}{[abs(N_{randn})]^{\frac{1}{\beta}}} \right) \tag{16}$$

$$\delta = \left\{ \frac{\Gamma(1+\beta) \times \sin\left(\frac{\pi}{2} \times \beta\right)}{\left[\Gamma\left(\frac{1+\beta}{2}\right) \times \beta \times 2^{\left(\frac{\beta-1}{2}\right)}\right]} \right\}^{\frac{1}{\beta}} \tag{17}$$

where $N_{randn}$, $\Gamma$, $\beta$, and $\delta$ denote the random number, gamma function, spatial exponent, and random value, respectively.

The effect of Fish Aggregating Devices (FADs) or eddy formation can influence the behaviors of the predators. The FADs function as local optimum that can easily trap the predators. To avoid stagnation and escape the influence of FADs, the predator or prey must take a long jump. Otherwise, it will get trapped in the local optimum. The effect of FADs is stated as:

$$\overrightarrow{Prey}_j = \begin{cases} \overrightarrow{Prey}_j + A\left[\overrightarrow{x}_{\min} + \overrightarrow{r} \otimes (\overrightarrow{x}_{\max} - \overrightarrow{x}_{\min})\right] \otimes \overrightarrow{u} & \text{if } r \leq \text{FADs} \\ \overrightarrow{Prey}_j + \left[\text{FADs}(1-r^1) + r^1\right] \left(\overrightarrow{Prey}_{r1} - \overrightarrow{Prey}_{r2}\right) & \text{if } r > \text{FADs} \end{cases} \tag{18}$$

where $r^1$ is a random number, and $\overrightarrow{x}_{\min}$ and $\overrightarrow{x}_{\max}$ denote the vectors containing the lower bound and upper bound of the dimensions. *r1* and *r2* are random indexes of the prey matrix. $\overrightarrow{u}$ is a range random vector that is less than the FAD coefficient probability value which is 0.2. The basic steps of the AMPA are summarized in the flowchart shown in Figure 2.

## 4. RESULT AND DISCUSSION

AMPA has been implemented extensively to find the optimal excitation amplitude among the array elements of the nonuniform 3-ring CCAA design. The results obtained by AMPA are benchmarked with six other metaheuristic algorithms namely, arithmetic optimization algorithm (AOA), moth flame

**Table 1.** The algorithms' parameter setting.

| Algorithm | Parameters | Values |
|---|---|---|
| AOA | $\alpha, \mu$, and Spiral constant | [5, 0.499, 1] |
| | Maximum MOP and minimum MOP | [1, 0.2] |
| MFO | Convergence constant | $[-1, -2]$ |
| | Random number range | $[-1, 1]$ |
| IWO | Minimum and Maximum seeds | [0, 5] |
| | Initial and Final standard deviation | [0.01, 0.1] |
| GWO | Control parameter | [2, 0] |
| NMPA | FADs and C | [0.2, 0.5] |
| MPA | FADs and C | [0.2, 0.5] |
| AMPA | learning coefficients $b_1$ and $b_2$ | 1.7 |
| | FADs and C | [0.2, 0.4] |

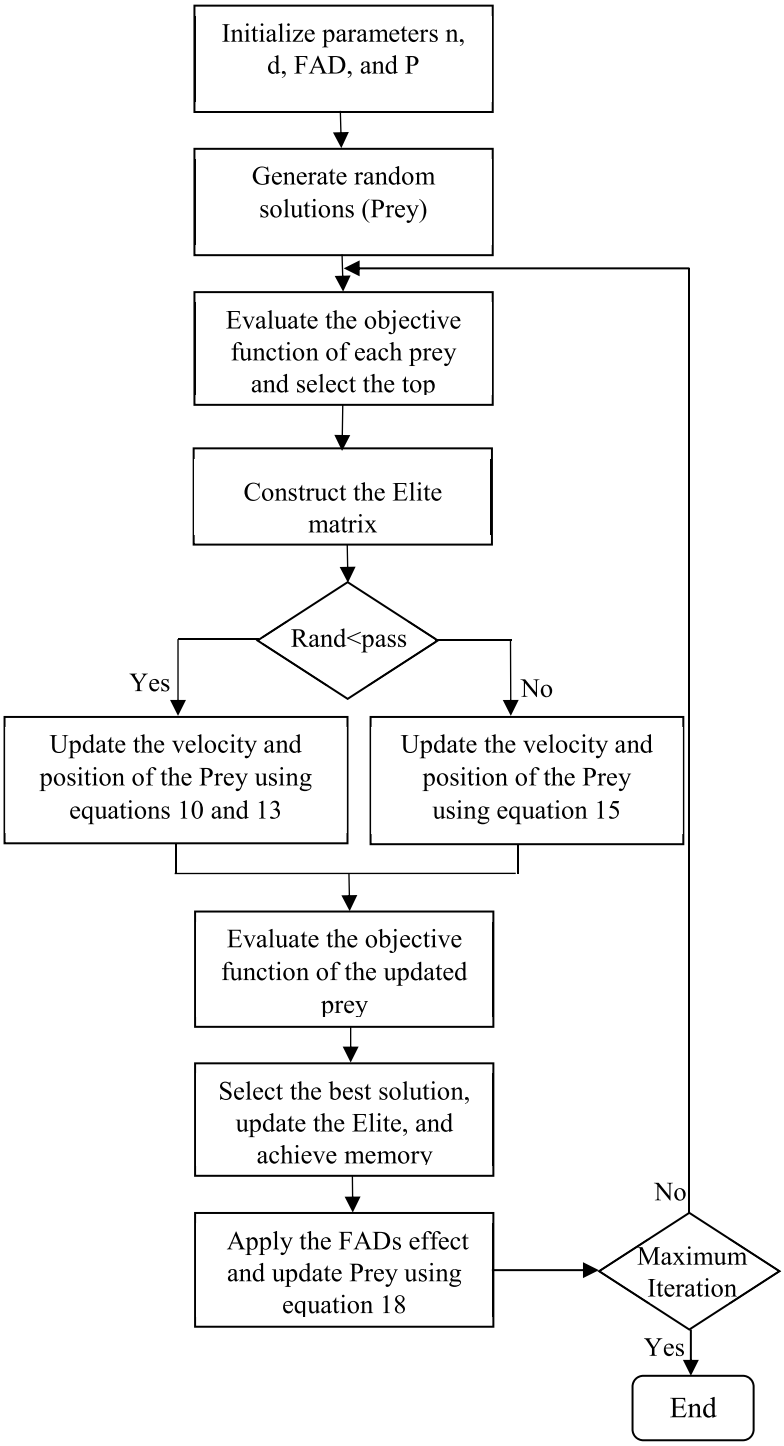


**Figure 2.** Flowchart for AMPA.

optimization (MFO) algorithm, invasive weed optimization (IWO) algorithm, grey wolf optimization (GWO), nonlinear marine predator algorithm (NMPA), and marine predator algorithm (MPA), and their control parameters are shown in Table 1. The population size, maximum iteration, and number of runs for each algorithm are set as 50, 100, and 50, respectively. The simulations are performed on MATLAB 2020a version with 16 GB RAM 11th Gen Intel(R) Core (TM) i7-11370H @ 3.30 GHz computer, and the best results are reported in this work.

### 4.1. CASE 1 — Optimization of Nonuniform CCAA with No Centre Element

In the first instance, the amplitude optimization of two different examples of three-ring CCAA with no centre element was performed using Equation (4). The first example is when $N_1 = 4$, $N_2 = 6$, $N_3 = 8$, and the second example is when $N_1 = 8$, $N_2 = 10$, and $N_3 = 12$. The inter-element spacing for the first example was set to $0.50\lambda$, $0.58\lambda$, and $0.77\lambda$, respectively, while for the second example, it was set to $0.55\lambda$, $0.615\lambda$, and $0.75\lambda$. The obtained SLL and FNBW for the first and second examples are presented in Table 2. Their radiation patterns and convergence curves are shown in Figures 3 and 4. Also, the excitation current that yields the SLL result for the AMPA is presented in Table 3. For the first example, AMPA attained a minimum SLL of 37.60 dB and FNBW of 80.40°. It obtained the best SLL value amongst the algorithms adopted with an FNBW which is much narrower than the uniform array. The SLL result of −28.7889°C obtained by AMPA for the second example shows that it outperformed MPA, NMPA, AOA, MFO, GWO, IWO, and the uniform array by 2.9554 dB, 1.5430 dB, 8.1043 dB, 3.0197 dB, 10.8445 dB, 4.3284 dB, and 19.2271 dB, respectively. Based on the optimization results of AMPA obtained for the first case, AMPA effectively reduces the SLL and obtains a very narrow FNBW, though it has the highest computational time which is due to the complexity of the algorithm. This outstanding result achieved by AMPA is due to its ability to escape local optima and explore larger search space.

**Table 2.** Optimization result obtained for Case-1 examples.

| 4,6,8-ELEMENT | | | | 8,10,12-ELEMENT | | | |
|---|---|---|---|---|---|---|---|
| Algorithm | Peak SLL (dB) | FNBW (°) | Time (s) | Algorithm | Peak SLL (dB) | FNBW (°) | Time (s) |
| Uniform | −11.2332 | 90.40 | | Uniform | −9.5593 | 55.20 | |
| IWO | −31.8575 | 83.60 | 1.73 | IWO | −24.4580 | 53.20 | 2.37 |
| GWO | −18.7121 | 76.80 | 1.81 | GWO | −17.9419 | 46.40 | 2.51 |
| MFO | −35.1021 | 90.40 | 1.75 | MFO | −25.7667 | 51.60 | 2.47 |
| AOA | −23.3269 | 85.60 | 1.77 | AOA | −20.6821 | 52.80 | 2.49 |
| NMPA | −35.6456 | 80.80 | 3.47 | NMPA | −27.2434 | 52.40 | 4.79 |
| MPA | −36.9822 | 82.40 | 2.98 | MPA | −25.8310 | 50.80 | 4.79 |
| AMPA | −37.6000 | 80.40 | 3.65 | AMPA | −28.7864 | 52.80 | 4.89 |

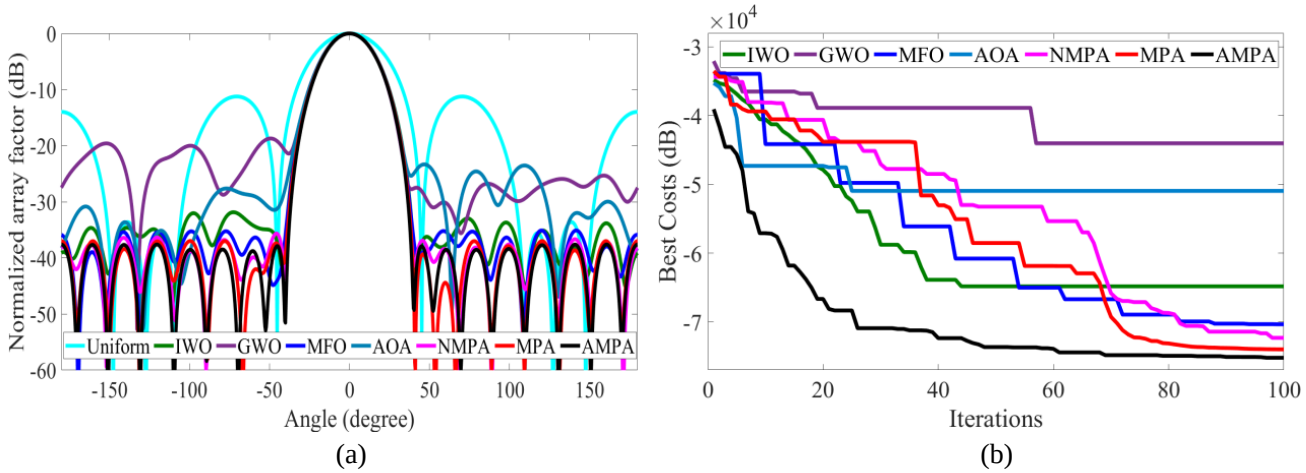


**Figure 3.** Plots showing the (a) radiation pattern and (b) convergence curve of 4,6,8 CCAA without centre element.

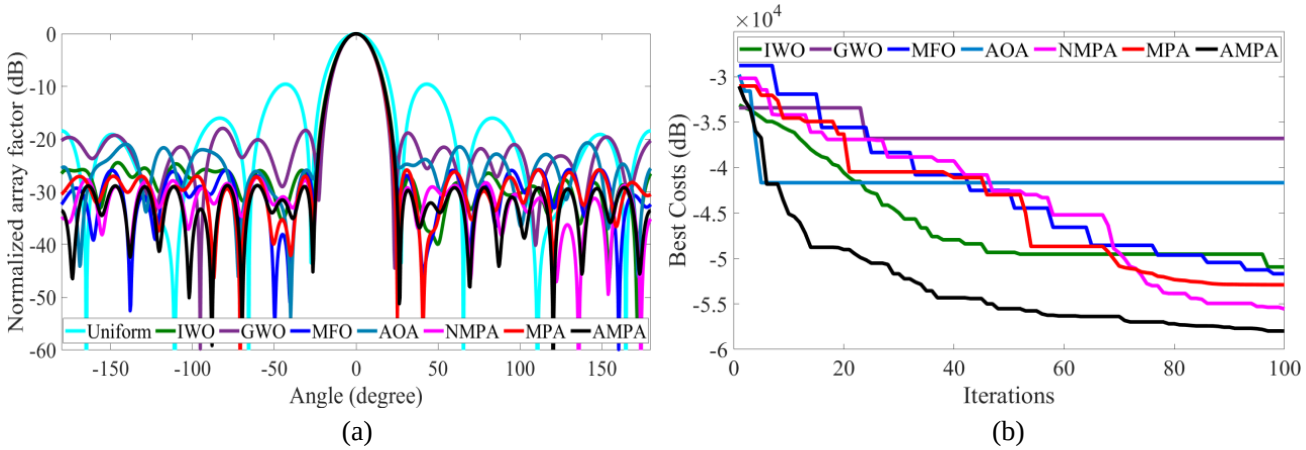


**Figure 4.** Plots showing the (a) radiation pattern and (b) convergence curve of 8,10,12 CCAA without centre element.

**Table 3.** Current excitations obtained by AMPA for Case-1.

| CASE-1 | Amplitude | | | | | | | | | |
|---|---|---|---|---|---|---|---|---|---|---|
| Example 1 | 0.9972 | 0.9163 | 1.0000 | 0.8866 | 0.7871 | 0.7970 | 0.9822 | 0.8010 | 0.7854 | |
| | 0.9970 | 0.6033 | 0.9974 | 0.6122 | 0.3243 | 0.6076 | 0.9933 | 0.5980 | 0.3487 | |
| Example 2 | 0.6987 | 0.5741 | 0.6805 | 0.9809 | 0.8986 | 0.3516 | 0.9340 | 0.9885 | 0.7252 | 0.1838 |
| | 0.1738 | 0.6313 | 0.5275 | 0.7817 | 0.0307 | 0.0308 | 0.7911 | 0.5600 | 0.4677 | 0.2990 |
| | 1.0000 | 0.2240 | 0.4854 | 0.5400 | 0.4064 | 0.4519 | 0.9873 | 0.4597 | 0.3823 | 0.4920 |

### 4.2. CASE 2 — Optimization of Nonuniform CCAA with a Centre Element

The second instance considered in this work is the amplitude optimization of $N_1 = 4$, $N_2 = 6$, $N_3 = 8$ and $N_1 = 8$, $N_2 = 10$, $N_3 = 10$ three-ring CCAA with a centre element using Equation (4). The 4,6,8 CCAA is named as example 3 while the 8,10,12 CCAA is named as example 4. For example 3, the inter-element spacing is set to $0.52\lambda$, $0.53\lambda$, and $0.68\lambda$, respectively. The SLL of $-44.4602$ dB, $-38.3823$ dB, $-39.6563$ dB, $-25.1988$ dB, $-33.3612$ dB, $-20.7311$ dB, $-29.5781$ dB was achieved by AMPA, MPA, NMPA, AOA, MFO, GWO, and IWO, respectively, as shown in Table 4 and Figure 5. In the fourth

**Table 4.** Optimization result obtained for Case-2 examples.

| 4,6,8-ELEMENT | | | | 8,10,12-ELEMENT | | | |
|---|---|---|---|---|---|---|---|
| Algorithm | Peak SLL (dB) | FNBW (°) | Time (s) | Algorithm | Peak SLL (dB) | FNBW (°) | Time (s) |
| Uniform | −12.3146 | 95.20 | – | Uniform | −10.7612 | 56.80 | – |
| IWO | −29.5781 | 102.00 | 1.48 | IWO | −28.4066 | 58.80 | 2.88 |
| GWO | −20.7311 | 96.80 | 1.56 | GWO | −18.9455 | 53.60 | 2.84 |
| MFO | −33.3612 | 98.80 | 1.48 | MFO | −26.7529 | 60.00 | 2.81 |
| AOA | −25.1988 | 112.40 | 1.51 | AOA | −22.6324 | 65.20 | 2.83 |
| NMPA | −39.6563 | 103.60 | 3.34 | NMPA | −30.3387 | 58.80 | 5.48 |
| MPA | −38.3823 | 105.20 | 3.31 | MPA | −30.1900 | 57.20 | 5.45 |
| AMPA | −44.3602 | 101.60 | 3.38 | AMPA | −34.0188 | 60.80 | 5.55 |

example, the inter-element spacing is set to $0.54\lambda$, $0.606\lambda$, and $0.72\lambda$, respectively, and it attained an SLL of $-34.0188$ dB, $-30.1900$ dB, $-30.3387$ dB, $-22.6324$ dB, $-26.7529$ dB, $-18.9455$ dB, $-28.4066$ dB for AMPA, MPA, NMPA, AOA, MFO, GWO, and IWO, respectively, as shown in Table 4. The radiation pattern and convergence curve of the third and fourth examples are shown in Figures 5 and 6. It is obvious that the improvements made to the standard MPA make the AMPA outperform all other algorithms in these examples. It is also observed that the FNBWs acquired by most of the algorithms in the Case-2 examples are a bit larger than that of the uniform array. This is due to the tradeoff between the SLL suppression and FNBW, and the lower the SLL is, the wider the FNBW is. However,

**Table 5.** Current excitations obtained by AMPA for Case-2.

| CASE-1 | Amplitude | | | | | | | | | | |
|---|---|---|---|---|---|---|---|---|---|---|---|
| Example 3 | 0.9002 | 0.3168 | 0.6194 | 0.3110 | 0.6320 | 0.9993 | 0.9992 | 0.9534 | 0.9981 | 1.0000 | |
| | 0.9290 | 0.4938 | 0.4404 | 0.5082 | 0.0171 | 0.5096 | 0.4353 | 0.4954 | 0.0029 | | |
| Example 4 | 0.9751 | 0.3876 | 0.9823 | 0.4022 | 0.9800 | 0.3728 | 0.9939 | 0.3208 | 1.0000 | 0.8972 | 0.0702 |
| | 0.0981 | 0.8879 | 0.9807 | 1.0000 | 0.0987 | 0.0860 | 0.9826 | 0.9972 | 0.4397 | 0.4076 | 0.7150 |
| | 0.3956 | 0.4410 | 0.3791 | 0.4516 | 0.4303 | 0.7967 | 0.3868 | 0.4906 | 0.3943 | | |

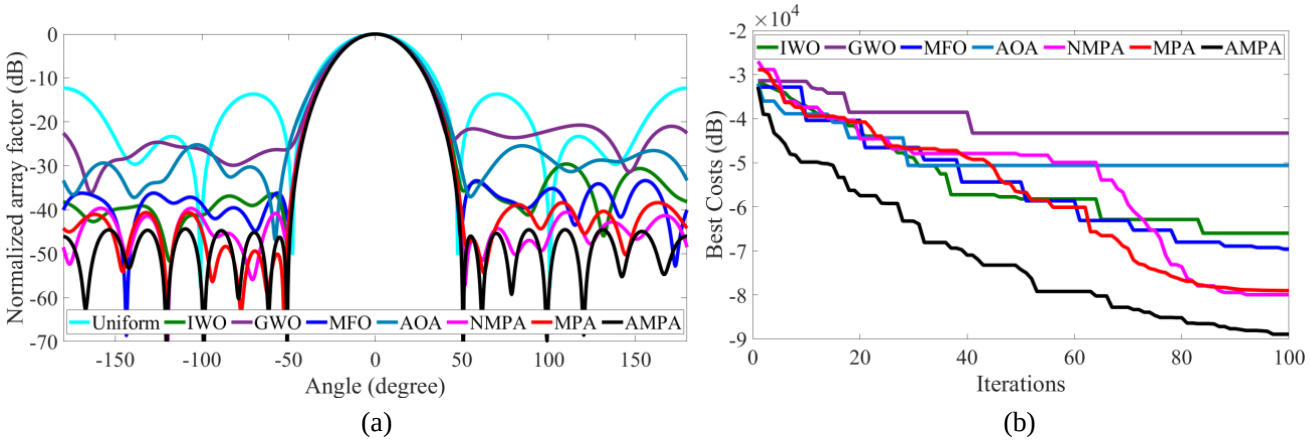


(a) (b)

**Figure 5.** Plots showing the (a) radiation pattern and (b) convergence curve of 4,6,8 CCAA with the centre element.

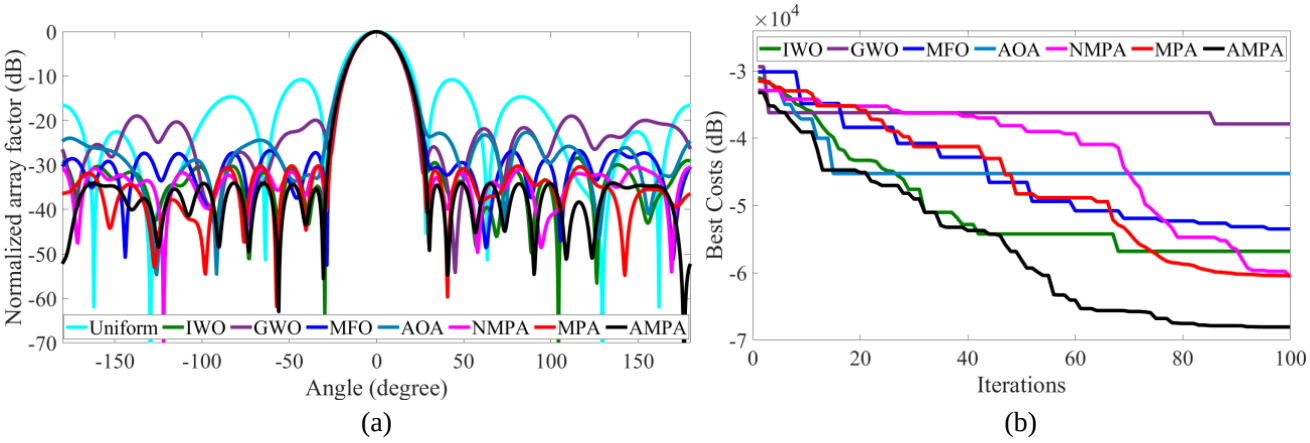


(a) (b)

**Figure 6.** Plots showing the (a) radiation pattern and (b) convergence curve of 8,10,12 CCAA with the centre element.

the FNBW is just a few degrees more than the uniform array, which is still considerable. The amplitude currents attained by AMPA for examples 3 and 4 are shown in Table 5.

### 4.3. Stability Test

The stochastic nature of metaheuristic algorithms warrants different optimization results in each independent run when the mathematical problems are solved; therefore, it is essential to conduct statistical tests to compare the efficacy of these algorithms. In this work, the stability performances of the AMPA and other algorithms adopted for the optimization of the CCAAs are tested. The stability test is conducted on the results (best costs) obtained during the optimization of the four examples of the CCAA considered in this work. Since the optimization is carried out for 50 independent runs, and 100 iterations are conducted in each run, each algorithm has 50 results used to estimate the best cost, worst cost, mean cost, and standard deviation of the results obtained. The estimated results are shown in Figures 7(a), 7(b), 7(c), and 7(d), for example 1, example 2, example 3, and example 4, respectively. Tables 6 and 7 further give the breakdown of the statistical result.

In terms of the best costs and average cost, AMPA has the top score among the algorithms for all four CCAA examples, and its standard deviation compares favourably with other algorithms. According to the figures and tables, the proposed AMPA algorithm achieves the overall best performance.

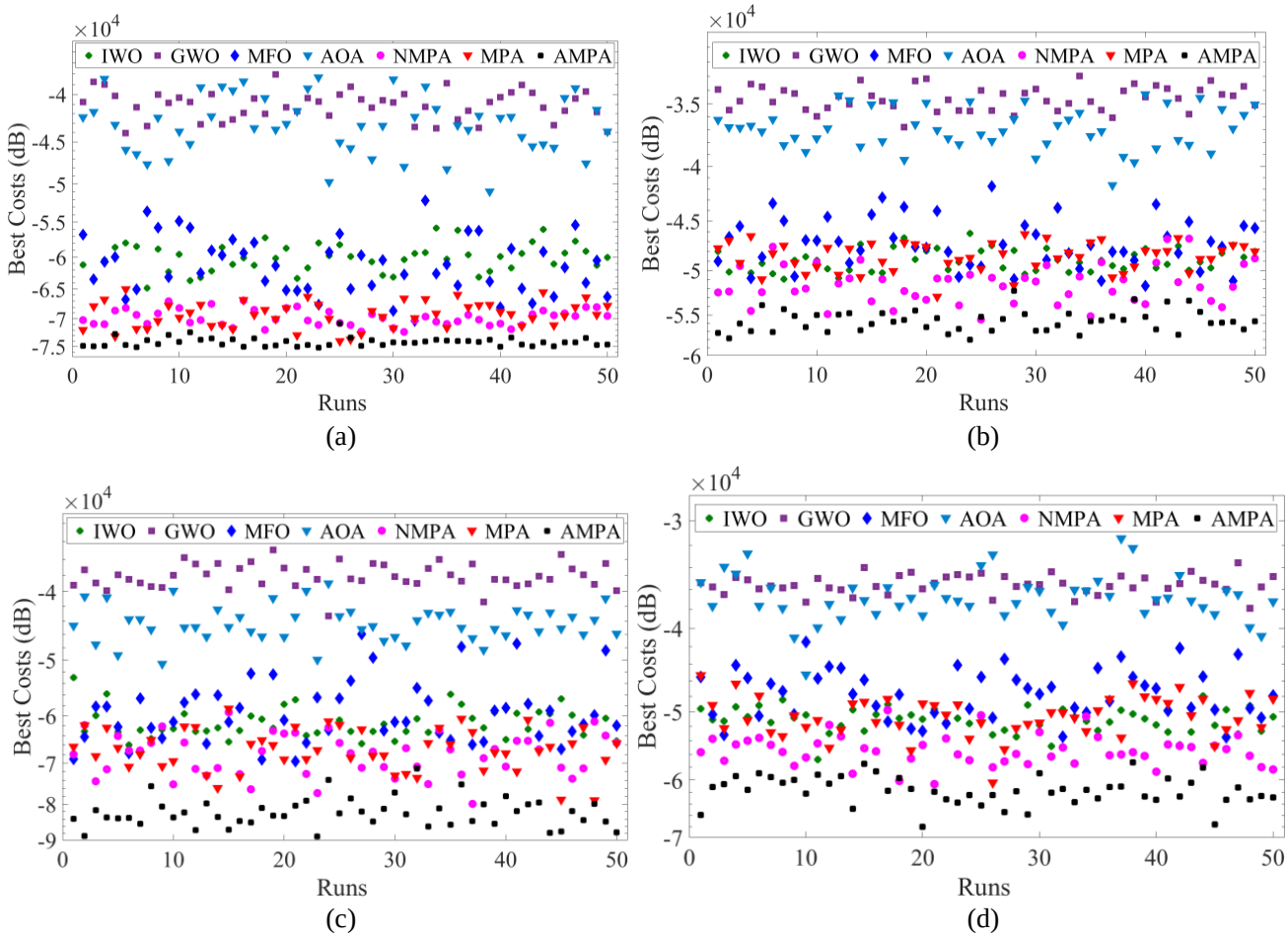


**Figure 7.** Plots showing the stability test (a) Example 1, (b) Example 2, (c) Example 3, (d) Example 4.

**Table 6.** Statistical result for case 1 (Example 1 and Example 2).

| Algorithms | 4,6,8-ELEMENT (Example 1) | | | | 8,10,12-ELEMENT (Example 2) | | | |
|---|---|---|---|---|---|---|---|---|
| | Best cost | Worst cost | Average cost | Standard deviation | Best cost | Worst cost | Average cost | Standard deviation |
| IWO | −6.48E+04 | −5.58E+04 | −6.02E+04 | 2.09E+03 | −5.09E+04 | −4.62E+04 | −4.90E+04 | 1.16E+03 |
| GWO | −4.40E+04 | −3.81E+04 | −4.11E+04 | 1.47E+03 | −3.68E+04 | −3.30E+04 | −3.46E+04 | 8.81E+02 |
| MFO | −7.04E+04 | −5.21E+04 | −6.15E+04 | 4.29E+03 | −5.17E+04 | −4.18E+04 | −4.73E+04 | 2.48E+03 |
| AOA | −5.10E+04 | −3.83E+04 | −4.33E+04 | 3.12E+03 | −4.17E+04 | −3.43E+04 | −3.70E+04 | 1.63E+03 |
| NMPA | −7.23E+04 | −6.69E+04 | −6.98E+04 | 1.39E+03 | −5.55E+04 | −4.67E+04 | −5.16E+04 | 2.13E+03 |
| MPA | −7.40E+04 | −6.50E+04 | −6.93E+04 | 2.26E+03 | −5.29E+04 | −4.63E+04 | −4.86E+04 | 1.49E+03 |
| AMPA | −7.52E+04 | −7.08E+04 | −7.42E+04 | 8.27E+02 | −5.80E+04 | −5.22E+04 | −5.57E+04 | 1.26E+03 |

**Table 7.** Statistical result for case 2 (Example 3 and Example 4).

| Algorithms | 4,6,8-ELEMENT (Example 3) | | | | 8,10,12-ELEMENT (Example 4) | | | |
|---|---|---|---|---|---|---|---|---|
| | Best cost | Worst cost | Average cost | Standard deviation | Best cost | Worst cost | Average cost | Standard deviation |
| IWO | −6.60E+04 | −5.30E+04 | −6.15E+04 | 2.83E+03 | −5.68E+04 | −4.79E+04 | −5.12E+04 | 1.71E+03 |
| GWO | −4.33E+04 | −3.49E+04 | −3.81E+04 | 1.54E+03 | −3.79E+04 | −3.35E+04 | −3.56E+04 | 9.13E+02 |
| MFO | −6.96E+04 | −4.60E+04 | −5.97E+04 | 5.81E+03 | −5.35E+04 | −4.15E+04 | −4.78E+04 | 3.12E+03 |
| AOA | −5.06E+04 | −3.89E+04 | −4.45E+04 | 2.55E+03 | −4.53E+04 | −3.14E+04 | −3.69E+04 | 2.39E+03 |
| NMPA | −7.99E+04 | −5.93E+04 | −6.83E+04 | 4.75E+03 | −6.07E+04 | −4.98E+04 | −5.55E+04 | 2.28E+03 |
| MPA | −7.90E+04 | −5.86E+04 | −6.72E+04 | 4.68E+03 | −6.04E+04 | −4.53E+04 | −5.07E+04 | 2.80E+03 |
| AMPA | −8.89E+04 | −7.13E+04 | −8.24E+04 | 3.80E+03 | −6.81E+04 | −5.72E+04 | −6.18E+04 | 2.39E+03 |

## 5. CONCLUSION

In this paper, the advanced marine predator algorithm (AMPA) is implemented to determine the optimal radiation pattern of the non-uniform 3-ring CCAA in the presence and absence of a centre element. AMPA introduces two unique factors to enhance the exploration and exploitation capability of the conventional MPA and improve the convergence rate: an improved velocity update strategy and a chaotic sequence parameter. This makes it especially suitable for solving the CCAA optimization problem. For the synthesis of the nonuniform 3-ring CCAA without a centre element, AMPA obtained an SLL result of −37.6000 dB and −28.7864 dB for 4,6,8-element CCAA and 8,10,12-element CCAA. Also, in the presence of a centre element, it obtained an SLL of −44.3602 dB and −34.0188 dB for the 4,6,8-element CCAA and 8,10,12-element CCAA, respectively. The stability test likewise proves that AMPA has a good level of stability as compared with other algorithms. The overall simulation results show that the AMPA performs better than MPA, NMPA, AOA, MFO, GWO, and IWO. This outstanding performance shows that AMPA can be employed effectively for the design of a 3-ring CCAA structure. A practical antenna array design can be made and fabricated based on the information provided in this work to meet optimal communication system needs.

## ACKNOWLEDGMENT

This work was supported by the National Natural Science Foundation of China (No. 42075129), Hebei Province Natural Science Foundation (No. E2021202179), Key Research and Development Project from Hebei Province (No. 19210404D, No. 20351802D, No. 21351803D).

## REFERENCES


1. Balanis, C. A., *Antenna Theroy: Analysis and Design*, 2012.
2. Bera, R., K. Kundu, and N. N. Pathak, "Optimal pattern synthesis of thinned and non-uniformly excited concentric circular array antennas using hybrid GSA-PSO technique," *Radioengineering*, Vol. 27, No. 2, 369–385, Jun. 2019, doi: 10.13164/re.2019.0369.
3. Amaireh, A. A., A. S. Al-Zoubi, and N. I. Dib, "Sidelobe-level suppression for circular antenna array via new hybrid optimization algorithm based on antlion and grasshopper optimization algorithms," *Progress In Electromagnetics Research C*, Vol. 93, 49–63, 2019.
4. Durmus, A. and R. Kurban, "Optimal synthesis of concentric circular antenna arrays using political optimizer," *IETE J. Res.*, Vol. 68, No. 1, 768–777, Jan. 2022, doi: 10.1080/03772063.2021.1902871.
5. Wang, T., K.-W. Xia, H.-L. Tang, S.-W. Zhang, and M. Sandrine, "A modified wolf pack algorithm for multiconstrained sparse linear array synthesis," *Int. J. Antennas Propag.*, Vol. 2020, No. 9483971, 1–12, Jan. 2020, doi: 10.1155/2020/9483971.
6. Liu, J., Z. Zhao, K. Yang, and Q. H. Liu, "A hybrid optimization for pattern synthesis of large antenna arrays," *Progress In Electromagnetics Research*, Vol. 145, 81–91, 2014.
7. Owoola, E. O., K. Xia, T. Wang, A. Umar, and R. G. Akindele, "Pattern synthesis of uniform and sparse linear antenna array using mayfly algorithm," *IEEE Access*, Vol. 9, 1–22, 2021, doi: 10.1109/ACCESS.2021.3083487.
8. Owoola, E. O., K. Xia, S. Ogunjo, S. Mukase, and A. Mohamed, "Advanced marine predator algorithm for circular antenna array pattern synthesis," *Sensors*, Vol. 22, No. 15, 5779, Aug. 2022, doi: 10.3390/s22155779.
9. Mandal, D., S. P. Ghoshal, and A. K. Bhattacharjee, "Optimal design of concentric circular antenna array using particle swarm optimization with constriction factor approach," *Int. J. Comput. Appl.*, Vol. 1, No. 17, 112–116, 2010, doi: 10.5120/353-534.
10. Guney, K., A. Durmus, and S. Basbug, "Backtracking search optimization algorithm for synthesis of concentric circular antenna arrays," *Int. J. Antennas Propag.*, Vol. 2014, 2014, doi: 10.1155/2014/250841.
11. Ram, G., D. Mandal, R. Kar, and S. P. Ghoshal, "Circular and concentric circular antenna array synthesis using cat swarm optimization," *IETE Tech. Rev.*, Vol. 32, No. 3, 204–217, 2015, doi: 10.1080/02564602.2014.1002543.
12. Ram, G., D. Mandal, R. Kar, and S. P. Ghoshal, "Directivity improvement and optimal far field pattern of time modulated concentric circular antenna array using hybrid evolutionary algorithms," *Int. J. Microw. Wirel. Technol.*, Vol. 9, No. 1, 177–190, 2017, doi: 10.1017/S1759078715001075.
13. Ram, G., D. Mandal, R. Kar, and S. P. Ghoshal, "Opposition-based BAT algorithm for optimal design of circular and concentric circular arrays with improved far-field radiation characteristics," *Int. J. Numer. Model. Electron. Networks, Devices Fields*, Vol. 30, No. 3–4, e2087, May 2017, doi:10.1002/jnm.2087.
14. Babayigit, B., "Synthesis of concentric circular antenna arrays using dragonfly algorithm," *Int. J. Electron.*, Vol. 105, No. 5, 784–793, May 2018, doi: 10.1080/00207217.2017.1407964.
15. Das, A., D. Mandal, S. P. Ghoshal, and R. Kar, "Concentric circular antenna array synthesis for side lobe suppression using moth flame optimization," *AEU — Int. J. Electron. Commun.*, Vol. 86, 177–184, Mar. 2018, doi: 10.1016/j.aeue.2018.01.017.
16. Dib, N., "Design of planar concentric circular antenna arrays with reduced side lobe level using symbiotic organisms search," *Neural Comput. Appl.*, Vol. 30, No. 12, 3859–3868, Dec. 2018, doi: 10.1007/s00521-017-2971-2.
17. Sun, G., Y. Liu, Z. Chen, S. Liang, A. Wang, and Y. Zhang, "Radiation beam pattern synthesis of concentric circular antenna arrays using hybrid approach based on cuckoo search," *IEEE Trans. Antennas Propag.*, Vol. 66, No. 9, 4563–4576, 2018, doi: 10.1109/TAP.2018.2846771.

18. Ismaiel, A. M., E. Elsaidy, Y. Albagory, H. A. Atallah, A. B. Abdel-Rahman, and T. Sallam, "Performance improvement of high altitude platform using concentric circular antenna array based on particle swarm optimization," *AEU — Int. J. Electron. Commun.*, Vol. 91, 85–90, Jul. 2018, doi: 10.1016/j.aeue.2018.05.002.
19. Das, A., D. Mandal, S. P. Ghoshal, and R. Kar, "An optimal mutually coupled concentric circular antenna array synthesis using ant lion optimization," *Ann. Telecommun.*, Vol. 74, Nos. 11–12, 687–696, Dec. 2019, doi: 10.1007/s12243-019-00729-3.
20. Jamunaa, D., F. N. Hasoon, and G. K. Mahanti, "Symbiotic organisms search optimisation algorithm for synthesis of phase-only reconfigurable concentric circular antenna array with uniform amplitude distribution," *Int. J. Electron. Lett.*, Vol. 8, No. 4, 460–471, Oct. 2020, doi: 10.1080/21681724.2019.1636294.
21. Faramarzi, A., M. Heidarinejad, S. Mirjalili, and A. H. Gandomi, "Marine predators algorithm: A nature-inspired metaheuristic," *Expert Syst. Appl.*, Vol. 152, 113377, Aug. 2020, doi: 10.1016/j.eswa.2020.113377.
22. Chen, X., X. Qi, Z. Wang, C. Cui, B. Wu, and Y. Yang, "Fault diagnosis of rolling bearing using marine predators algorithm-based support vector machine and topology learning and out-of-sample embedding," *Measurement*, Vol. 176, 2020, 109116, May 2021, doi: 10.1016/j.measurement.2021.109116.
23. Chen, G., Y. Xiao, F. Long, X. Hu, and H. Long, "An Improved marine predators algorithm for short-term hydrothermal scheduling," *IAENG Int. J. Appl. Math.*, Vol. 51, No. 4, 1–14, 2021.
24. Ramezani, M., D. Bahmanyar, and N. Razmjooy, "A new improved model of marine predator algorithm for optimization problems," *Arab. J. Sci. Eng.*, Vol. 46, No. 9, 8803–8826, 2021, doi: 10.1007/s13369-021-05688-3.
25. Bouchekara, H., "Solution of the optimal power flow problem considering security constraints using an improved chaotic electromagnetic field optimization algorithm," *Neural Comput. Appl.*, Vol. 32, No. 7, 2683–2703, Apr. 2020, doi: 10.1007/s00521-019-04298-3.